Published in final edited form as:
J Heart Lung Transplant. 2014 April ; 33(4): 372–381. doi:10.1016/j.healun.2014.01.866.

ASSESSMENT OF MYOCARDIAL VIABILITY AND LEFT VENTRICULAR FUNCTION IN PATIENTS SUPPORTED BY A LEFT VENTRICULAR ASSIST DEVICE

Deepak K. Gupta, MD[1], **Hicham Skali, MD MSc**[1], **Jose Rivero, MD**[1], **Patricia Campbell, MD**[3], **Leslie Griffin, APRN**[1], **Colleen Smith, APRN**[1], **Courtney Foster, CNMT**[2], **Brian Claggett, PhD**[1], **Robert J. Glynn, PhD**[4], **Gregory Couper, MD**[1], **Michael M. Givertz, MD**[1], **Mandeep R. Mehra, MD**[1], **Marcelo Di Carli, MD**[1,2], **Scott D. Solomon, MD**[1], and **Marc A Pfeffer, MD PhD**[1]

[1]Cardiovascular Division, Department of Medicine, Brigham and Women's Hospital, Harvard Medical School, Boston, MA, United States

[2]Division of Nuclear Medicine and Molecular Imaging, Department of Radiology, Brigham and Women's Hospital, Harvard Medical School, Boston, MA, United States

[3]Department of Cardiac Sciences, University of Calgary, Canada

[4]Department of Biostatistics, Brigham and Women's Hospital, Harvard Medical School, Boston, MA, United States

Abstract

Background—Chronically supported left ventricular assist device (LVAD) patients may be candidates for novel therapies aimed at promoting reverse remodeling and myocardial recovery. However, the impact of hemodynamic unloading with a LVAD on myocardial viability and LV function in chronically supported LVAD patients has not been fully characterized. We aimed to develop a non-invasive imaging protocol to serially quantify native cardiac structure, function, and myocardial viability while at reduced LVAD support.

Methods—Clinically stable (n=18) ambulatory patients supported by a HeartMate II LVAD (median age 61 yrs, 83% men, median durations of heart failure 4.6 years and LVAD support 7 months) were evaluated by echocardiography and ^{99m}Tc-Sestamibi SPECT imaging at baseline and after a 2–3 month interval. Echocardiographic measures of LV size and function, including speckle tracking derived circumferential strain, were compared between ambulatory and reduced LVAD support at baseline and between baseline and follow up at reduced LVAD support. The extent of myocardial viability by SPECT was compared between baseline and follow up at reduced LVAD support.

Results—With reduction in LVAD speeds (6600 RPM, IQR: 6200,7400), LV size increased, LV systolic function remained stable, and filling pressures nominally worsened. After a median 2.1

Address Correspondence to: Marc A Pfeffer, MD PhD Brigham and Women's Hospital, Cardiovascular Division 75 Francis Street, Boston, MA 02115 Tele: (617) 732-5681 Fax: (617) 732-5291 mpfeffer@partners.org.

Disclosures MRM reports consulting fees from Thoratec. In addition MRM consults for the NHLBI as Chairman of the DSMB for the REVIVE-IT study.

months, on repeat imaging while at reduced LVAD speed, cardiac structure, function, and the extent of viable myocardium, both globally and regionally, was unchanged.

Conclusions—In clinically stable chronically supported LVAD patients, intrinsic cardiac structure, function, and myocardial viability did not significantly change over the pre-specified timeframe. Echocardiographic circumferential strain and ^{99m}Tc-Sestamibi SPECT myocardial viability imaging may provide useful non-invasive endpoints for the assessment of cardiac structure and function, particularly for phase II studies of novel therapies aimed at promoting reverse remodeling and myocardial recovery in LVAD patients.

Introduction

Implantations of left ventricular assist devices (LVAD) as a bridge to heart transplantation or lifetime (destination) therapy have been increasing (1). While LVADs improve survival in advanced heart failure (HF) (2, 3), sufficient myocardial recovery to allow LVAD explantation has also been reported, although pooled estimates indicate that recovery occurs in the minority (1–15%) of patients (1, 4–6). This emphasizes the importance of exploring therapeutic options in the broader LVAD population to reverse myocardial dysfunction and promote recovery (4–9). However, prior to the delivery of novel therapies, a basis for quantitatively assessing cardiac structure and function both under different loading conditions and over time in LVAD patients must first be ascertained (6, 10, 11).

Non-invasive imaging of cardiac structure and function is an important component in evaluating LVAD patients (10). Transthoracic echocardiography is the mainstay, due to its broad availability, ability to provide hemodynamic and valvular information, good spatial resolution, and lack of radiation (10, 12, 13). Nuclear imaging with ^{99m}Tc-Sestamibi SPECT is a well validated method for quantifying myocardial scar and offers complimentary information to that obtained with echocardiography (14, 15). Nuclear ^{123}I-MIBG imaging has also been utilized to demonstrate improvement in sympathetic innervation in the first 6 months following LVAD (16, 17). However, MIBG imaging does not allow regional quantification of fibrosis/scar, is not widely available, and is more time intensive than ^{99m}Tc-Sestamibi SPECT imaging. Additional benefits of ^{99m}Tc-Sestamibi include rapid tracer uptake, short SPECT imaging acquisition time (15–20 minute), wide availability, and validation as a robust method for assessing global and regional LV response to therapies, including stem cells (18, 19).

A universally agreed upon methodology for assessing cardiac structure and function in the LVAD population has not yet been established (11). Moreover, most prior studies on cardiac structure and function in LVAD patients have focused on the early period of hemodynamic unloading, i.e. the first 6 months post implantation (20, 21). Whether hemodynamic unloading in patients chronically supported by LVADs is associated with changes in cardiac structure and function has been less well characterized (22, 23). Therefore, in this report we describe a prospective non-invasive imaging protocol designed to evaluate serial measurements of cardiac structure, function, and myocardial viability at reduced LVAD support in stable outpatients chronically supported on a continuous flow axial LVAD.

Methods

Study population

Between December 1, 2011 and December 31, 2012, clinically stable outpatients supported on a HeartMate II (Thoratec Corp. Pleasanton, CA) LVAD who received their care at Brigham and Women's Hospital, Boston, MA, were approached to voluntarily participate in this imaging protocol (Figure 1). Patients who had their first LVAD implantation within the

preceding two years were eligible (n=60). Of these patients, twenty-eight were excluded (8 dead, 8 post cardiac transplant, 12 medically unstable). Of the thirty two stable ambulatory LVAD patients, nine did not provide consent, and five consented but were not imaged due to the development of medical instability or withdrawal of consent. The study population was comprised of 18 patients of whom 17 completed the entire protocol and one underwent cardiac transplantation after baseline, but before follow up. The Institutional Review Board approved the study and all imaged patients provided written informed consent.

Imaging Protocol

Patients were scheduled for two study visits (baseline and follow up) approximately 2-3 months apart. At each study visit, patients were evaluated in the dedicated LVAD clinic in the morning and then underwent transthoracic echocardiography and nuclear SPECT imaging in the afternoon. All patients were anticoagulated with warfarin and had an INR ≥ 1.5 on the day of imaging.

Comprehensive 2D, M-Mode, and Doppler echocardiography (GE Vivid 7, GE Healthcare, Waukesha, WI) was performed at ambulatory LVAD speeds. An optimization study with adjustments to LVAD speeds (±400 RPM) was performed as clinically indicated. Following this, the LVAD speed was reduced by 600–800 RPMs and after a 5 minute equilibration period, limited echocardiographic imaging was obtained. LVAD speed was sequentially reduced in this manner until full aortic valve opening was identified (defined as aortic valve cusp separation ≥2.0 cm by M-mode with every QRS complex). Once full aortic valve opening was identified, LVAD speeds were further reduced by 600–800 RPM or to 6000 RPM, whichever was higher, to ensure shifting of the balance of support from the LVAD to native cardiac function. For patients in whom full aortic valve opening was not achieved, LVAD speeds were reduced to 6000 RPM, as this has previously been demonstrated to be sufficient for assessing native cardiac function (20). At reduced LVAD speed, comprehensive echocardiography was repeated. Patients were monitored throughout by a nurse practitioner and cardiologist.

At reduced LVAD support, approximately 25mCi of ^{99m}Tc-Sestamibi were injected intravenously. The nuclear tracer was allowed to circulate for 10 minutes during reduced LVAD support, before returning to optimized ambulatory LVAD settings. Approximately 45 minutes after injection of the tracer, patients underwent gated ^{99m}Tc-Sestamibi SPECT imaging on a Symbia SPECT/CT (Siemens Corp., Malvern, PA).

Echocardiographic Analyses

Echocardiographic measures of cardiac structure and function were quantified offline using vendor independent software (TomTec, Unterschleißheim, Germany). Echocardiographic quantification was performed according to American Society of Echocardiography guidelines (24–26). Left ventricular (LV) function was assessed by fractional area change (13) and circumferential systolic strain by speckle tracking (Cardiac Performance Analysis, TomTec, Unterschleißheim, Germany) in the parasternal short axis view at the mid ventricular papillary muscle level (Figure 2) (27). Final values for all indices were taken as the mean of measurements from three cardiac cycles. In one patient, poor acoustic windows precluded quantification of LV fractional area change, circumferential strain, and right ventricular size and function.

^{99m}Tc-Sestamibi SPECT Analyses

LV viability was quantified using a commercially available software package (Corridor 4DM version 12, INVIA Corp., Ann Arbor, MI) using a seventeen segment model (28). The segments in which the LVAD cannula was present were excluded from analysis. A viable

segment was defined as one with >55% peak normalized counts (15, 28). The overall amount of viable myocardium was calculated as the average of the proportions of each segment in which peak counts were above the threshold of 55%, after excluding segments in which the LVAD cannula was present (Figure 3) (15, 29). The extent of viable LV myocardium was quantified in each patient at baseline and follow up. One patient was excluded from SPECT analyses due to artifact produced by bowel overlying the LV.

As novel therapies aimed at promoting reverse remodeling and augmenting myocardial recovery may be potentially delivered via an intracoronary route, peak normalized counts were also evaluated regionally. After excluding segments in which the LVAD cannula was present, those segments in which peak normalized counts were ≤55%, i.e. non-viable, were identified. If two or more contiguous segments within the same coronary distribution had peak normalized counts ≤55%, this non-viable territory was classified as a "target zone". If more than one target zone was identified in a patient, for example in multivessel coronary artery disease, then the target zone with the lowest average peak normalized counts was included (30, 31), such that each patient had no more than one target zone. The average of peak normalized counts in the segments comprising the target zone was calculated within each patient at baseline and follow up (Figure 4).

Correlation of echocardiographic LV function with ^{99m}Tc-Sestamibi SPECT myocardial viability

Using standardized segmentation of the six mid LV segments (anterior, anterolateral, inferolateral, inferior, inferoseptum, and anteroseptum), we assessed the relationship between systolic function from speckle tracking echocardiography and myocardial viability from ^{99m}Tc-Sestamibi SPECT (Figure 5) (28, 32). Apical and basal segments were not assessed due to the presence of the LVAD cannula and mitral valve, respectively. Each of the six mid LV segments was dichotomized as non-viable or viable, if peak normalized counts were ≤55% or > 55%, respectively. Average circumferential strain was calculated in non-viable and viable segments at both baseline and follow up.

Statistical Analyses

Echocardiographic measures of cardiac structure and function were compared between ambulatory vs. reduced LVAD support at baseline, as well as, between baseline and follow up at reduced LVAD support. The extent of LV viability was quantified by ^{99m}Tc-Sestamibi SPECT and was compared between baseline and follow up. Average peak normalized counts in the target zone was also calculated and compared between baseline and follow up. For correlation between LV function and myocardial viability, circumferential strain was quantified in non-viable and viable segments and compared between baseline and follow up. Summary statistics are presented as percentages or median (IQR) with comparisons via the Wilcoxon signed rank or rank sum test or Fisher's exact test, as appropriate. Two-sided p values <0.05 were considered significant. Intraclass correlation coefficients were calculated to assess for the consistency of imaging measures within patients from baseline to follow up. Analyses were performed using Stata 11.2 (Stata Corp., College Station, Texas).

Results

Study Population

Among the 18 imaged LVAD patients, the majority were men (83%), the median age was 61 years, and patients had HF for a median of 4.6 years (Table 1). The baseline study was performed approximately 7 months post LVAD implantation. Angiographic coronary artery disease was present in 10 (56%) patients and 2 (11%) patients had a history of cardiac sarcoidosis. All patients were taking warfarin and aspirin and nearly all patients had an

implantable cardioverter-defibrillator. Neurohormonal therapy and other cardiovascular medications were maintained at maximally tolerated doses without change at all study time points.

Cardiac structure and function at reduced LVAD support

LVAD speeds were decreased from ambulatory settings of 9200 (IQR: 9200,9600) RPMs to 6600 (IQR: 6200,7400) RPMs (Table 2). With decreasing LVAD support, there was a corresponding increase in pulsatility index, but no significant change in heart rate or Doppler blood pressure. Reduction of LVAD support was associated with an increase in LV size in both systole and diastole, although LV function, assessed by mid ventricular fractional area change and global circumferential strain, did not significantly change. In concert with the increase in LV size with reduction of LVAD support, right ventricular size decreased, although right ventricular function measured via fractional area change did not significantly change. With loading of the LV at reduced LVAD support, there were nominal changes in the direction of worsening filling pressures measured by E/e'. Importantly, no significant adverse events (e.g. arrhythmias, stroke/TIA, or heart failure) occurred during speed reduction. Furthermore, LVAD function (power and flow) was stable after returning to ambulatory settings.

Stability of cardiac structure, function, and myocardial viability over time at reduced LVAD support

After a median of 2.1 months, seventeen LVAD patients underwent follow up imaging of cardiac structure and function following the same protocol as at baseline. Cardiac structure and function while at reduced LVAD speed was compared between the baseline and follow up studies (Table 3). LVAD speeds and pulsatility index were similar between baseline and follow up at reduced support. Echocardiographic parameters of both LV and RV size and function at reduced LVAD support remained stable between baseline and follow up.

Therapies aimed at promoting reverse remodeling and myocardial recovery may have global or regional effects. Therefore, we evaluated both global and regional measures of LV viability with ^{99m}Tc-Sestamibi SPECT imaging. Between baseline and follow up, the extent of global LV viability measured by ^{99m}Tc-Sestamibi SPECT did not significantly change (median Δ 0.10%, IQR −1.7,2.2, p = 0.80; ICC 0.97, 95%CI 0.95,1.00) (Figure 3). Similarly, average peak normalized counts in the target zone supplied by a coronary artery remained stable between baseline and follow up (median Δ 0.10%, IQR −1.5,1.9, p = 0.88; ICC 0.96, 95%CI 0.93–1.00) (Figure 4).

Regional viability and left ventricular function at reduced LVAD support and over time

The relationship between systolic function from speckle tracking echocardiography and myocardial viability from ^{99m}Tc-Sestamibi SPECT we assessed in the six mid LV segments (Figure 5). Non-viable and viable segments were defined as those with ≤55% or >55% of peak normalized counts by ^{99m}Tc-Sestamibi SPECT imaging, respectively. Circumferential strain in non-viable and viable segments remained stable between baseline and follow up. In addition, circumferential strain was significantly more impaired in non-viable as compared to viable segments and this relationship was also unchanged between baseline and follow up.

Discussion

Sufficient myocardial recovery to allow LVAD explantation has been reported in a small minority and these patients have predominantly been younger with non-ischemic etiologies for HF, with reverse remodeling occurring early within the first 6 months of hemodynamic

unloading with LVADs (1, 4–6). The majority of LVAD patients do not sustain myocardial recovery and with the expanding LVAD population (1) a substantial number of patients may be candidates for novel therapies that promote reverse remodeling and augment myocardial recovery. However, there have been few pre-defined protocols for evaluating cardiac structure and function in LVAD patients (8, 20, 33, 34) resulting in a lack of standardization for the assessment of myocardial reverse remodeling and recovery (11).

By prospectively imaging cardiac structure, function, and viability under different loading conditions and over time in stable outpatients chronically supported on a HeartMate II LVAD, our findings may help establish a standardized protocol for assessment of these patients. As anticipated with reduction in LVAD speeds LV size increased, but without deterioration of LV systolic function. Importantly, in these clinically stable patients, imaging at reduced LVAD support was repeated after approximately 2 months and intrinsic ventricular cardiac structure, function, and the extent of viable myocardium, both globally and regionally, did not significantly change. Moreover, regional LV function was reproducibly related to the extent of viable myocardium both at baseline and follow up. These results demonstrate the feasibility and reproducibility of this non-invasive echocardiographic and ^{99m}Tc-Sestamibi SPECT imaging protocol for assessing cardiac structure, function, and viability in a chronically supported clinically stable LVAD population.

Cardiac structure and function at reduced LVAD support

The ability of the LVAD supported heart to maintain preserved structure and function under increased loading conditions may predict sustainable myocardial recovery (11). Short of LVAD explantation, the closest approximation to evaluating intrinsic myocardial function in LVAD patients is through “turn down” or “off-pump” studies during which the balance of work has been shifted from mechanical circulatory support to the native heart (10). Prior studies suggest that reduction of speed in the HeartMate II device to 6000 RPM effectively provides an “off-pump” study (8, 20). However, it has also been noted that the ability of the LV to generate sufficient force to open the aortic valve at high LVAD speeds (>10,000 RPM) in the setting of clinical stability and absence of LVAD malfunction may indicate myocardial recovery (13). In our protocol, we sequentially reduced LVAD speeds to evaluate for full aortic valve opening or 6000 RPM, whichever was higher. The range of LVAD speeds needed to complete this protocol was 6000–8000 RPMs, suggesting not only that most chronically supported LVAD patients are maintained at speeds to effectively decompress the LV, but also that most chronically supported LVAD patients do not have sufficient native cardiac function to overcome higher levels of LVAD support. Furthermore, at reduced LVAD speed we found that most patients were unable to maintain cardiac size and filling pressures, or augment systolic function in response to increased loading conditions, portending a low likelihood of sustainable myocardial recovery. These findings are consistent with previous reports at reduced LVAD support providing validity to this imaging approach (20, 35, 36).

Stability of cardiac structure, function, and viability at reduced LVAD support

Chronic hemodynamic unloading with LVAD support has been associated with improvement in cardiac structure and function in some patients (4, 37–43). Recently, several groups demonstrated that the extent of myocardial fibrosis is related to the potential for myocardial recovery in LVAD patients (44–47). ^{99m}Tc-Sestamibi SPECT has been previously validated for the non-invasive assessment of myocardial viability (32), and is highly correlated ($r = 0.89$, $p < 0.001$) with the extent of histologic fibrosis in an advanced HF population awaiting cardiac transplant (14). With this prospective non-invasive imaging protocol including ^{99m}Tc-Sestamibi SPECT, we found that in most patients with chronic

LVAD support, native cardiac viability, both globally and regionally, did not significantly change over time. While major changes in cardiac structure and function were not anticipated in chronically supported LVAD patients, these quantitative measures are important for planning future trials of novel therapies aimed at augmenting reverse remodeling and myocardial recovery. The demonstration that regional function was related to the extent of viable myocardium and that this relationship between nuclear assessed viability and echocardiographically assessed myocardial function at reduced LVAD support was also stable from baseline to follow up will also be important for any future studies trying to alter cardiac structure and function. These findings also suggest that speckle tracking echocardiography and ^{99m}Tc-Sestamibi imaging may be useful and complimentary non-invasive tools for assessing myocardial function and viability and potentially the response to therapies in chronically supported LVAD patients.

Limitations

While we present the feasibility of our standardized prospective non-invasive imaging protocol in chronically supported LVAD patients, limitations should be noted. We imaged a relatively small number of patients who were of older age and in which there was heterogeneity in etiology, as well as, durations of HF and LVAD support. We did not evaluate the early post LVAD period as chronically supported LVAD patients represent the majority of LVAD patients and therefore may be the most suitable candidates for evaluating novel therapies aimed at augmenting reverse remodeling and myocardial recovery. Patients were assessed over a relatively short duration of follow up during which neurohormonal antagonists were prescribed at maximally tolerated, though not necessarily target doses for heart failure (8). The 2–3 month time frame for follow up was pre-specified in order to 1) minimize loss to follow up due to intervening transplant or change in medical stability and 2) in anticipation of the time frame in which the effect of a novel therapy aimed at promoting reverse remodeling may be seen.

Not all patients had completely interpretable echocardiographic and/or SPECT images although only one patient was excluded from nuclear analysis and one from echocardiographic measures of strain. In addition, the presence of the LVAD cannula imparts challenges in imaging particularly of the apical segments, although we accounted for this in both the nuclear and echocardiographic protocols. We cannot exclude that the apical cannula may affect circumferential strain, perhaps due to tethering, which may vary based upon cannula position or orientation. However, as paired comparisons were made within each patient at reduced speed and over time, it would be expected the effect on circumferential strain due to the cannula should be similar in each patient. In addition, all imaged patients had the HeartMate II device, and therefore the findings may not apply to other types of LVADs, such as intrapericardial devices.

Conclusions

We prospectively evaluated cardiac structure, function, and viability under different loading conditions and over time in stable outpatients chronically supported on a HeartMate II LVAD. We found that intrinsic cardiac structure, function, and viability, both globally and regionally, did not significantly change over time. Echocardiography, in particular speckle tracking derived circumferential strain, and ^{99m}Tc-Sestamibi SPECT myocardial viability imaging may provide useful non-invasive endpoints for the assessment of cardiac structure in function, particularly for phase II studies of novel therapies aimed at promoting myocardial recovery in LVAD patients.

Acknowledgments

The authors thank the patients for their important contributions.

Funding Sources Support was provided by the National Institute of Health grant (5 P20 HL101866-02) to MAP. Support was also provided for DKG by the National Heart, Lung, and Blood Institute training grant (T32 HL094301-02) to MDC.

References

1. Kirklin JK, Naftel DC, Kormos RL, et al. Fifth INTERMACS annual report: risk factor analysis from more than 6,000 mechanical circulatory support patients. J Heart Lung Transplant. 2013; 32:141–56. [PubMed: 23352390]
2. Rose EA, Gelijns AC, Moskowitz AJ, et al. Long-term use of a left ventricular assist device for end-stage heart failure. N Engl J Med. 2001; 345:1435–43. [PubMed: 11794191]
3. Miller LW, Pagani FD, Russell SD, et al. Use of a continuous-flow device in patients awaiting heart transplantation. N Engl J Med. 2007; 357:885–96. [PubMed: 17761592]
4. Hall JL, Fermin DR, Birks EJ, et al. Clinical, molecular, and genomic changes in response to a left ventricular assist device. J Am Coll Cardiol. 2011; 57:641–52. [PubMed: 21292124]
5. Mann DL, Barger PM, Burkhoff D. Myocardial recovery and the failing heart: myth, magic, or molecular target? J Am Coll Cardiol. 2012; 60:2465–72. [PubMed: 23158527]
6. Drakos SG, Kfoury AG, Stehlik J, et al. Bridge to recovery: understanding the disconnect between clinical and biological outcomes. Circulation. 2012; 126:230–41. [PubMed: 22777666]
7. Maybaum S, Mancini D, Xydas S, et al. Cardiac improvement during mechanical circulatory support: a prospective multicenter study of the LVAD Working Group. Circulation. 2007; 115:2497–505. [PubMed: 17485581]
8. Birks EJ, George RS, Hedger M, et al. Reversal of severe heart failure with a continuous-flow left ventricular assist device and pharmacological therapy: a prospective study. Circulation. 2011; 123:381–90. [PubMed: 21242487]
9. Soppa GK, Barton PJ, Terracciano CM, Yacoub MH. Left ventricular assist device-induced molecular changes in the failing myocardium. Curr Opin Cardiol. 2008; 23:206–18. [PubMed: 18382208]
10. Estep JD, Chang SM, Bhimaraj A, Torre-Amione G, Zoghbi WA, Nagueh SF. Imaging for ventricular function and myocardial recovery on nonpulsatile ventricular assist devices. Circulation. 2012; 125:2265–77. [PubMed: 22566350]
11. Mann DL, Burkhoff D. Is myocardial recovery possible and how do you measure it? Curr Cardiol Rep. 2012; 14:293–8. [PubMed: 22437373]
12. Rasalingam R, Johnson SN, Bilhorn KR, et al. Transthoracic echocardiographic assessment of continuous-flow left ventricular assist devices. J Am Soc Echocardiogr. 2011; 24:135–48. [PubMed: 21236640]
13. Estep JD, Stainback RF, Little SH, Torre G, Zoghbi WA. The role of echocardiography and other imaging modalities in patients with left ventricular assist devices. JACC Cardiovasc Imaging. 2010; 3:1049–64. [PubMed: 20947051]
14. Medrano R, Lowry RW, Young JB, et al. Assessment of myocardial viability with 99mTc sestamibi in patients undergoing cardiac transplantation. A scintigraphic/pathological study. Circulation. 1996; 94:1010–7. [PubMed: 8790039]
15. Gibbons RJ, Miller TD, Christian TF. Infarct size measured by single photon emission computed tomographic imaging with (99m)Tc-sestamibi: A measure of the efficacy of therapy in acute myocardial infarction. Circulation. 2000; 101:101–8. [PubMed: 10618311]
16. George RS, Birks EJ, Cheetham A, et al. The effect of long-term left ventricular assist device support on myocardial sympathetic activity in patients with non-ischaemic dilated cardiomyopathy. Eur J Heart Fail. 2013; 15:1035–43. [PubMed: 23610136]
17. Drakos SG, Athanasoulis T, Malliaras KG, et al. Myocardial sympathetic innervation and long-term left ventricular mechanical unloading. JACC Cardiovasc Imaging. 2010; 3:64–70. [PubMed: 20129533]

18. Beeres SL, Bengel FM, Bartunek J, et al. Role of imaging in cardiac stem cell therapy. J Am Coll Cardiol. 2007; 49:1137–48. [PubMed: 17367656]
19. Grajek S, Popiel M, Gil L, et al. Influence of bone marrow stem cells on left ventricle perfusion and ejection fraction in patients with acute myocardial infarction of anterior wall: randomized clinical trial: Impact of bone marrow stem cell intracoronary infusion on improvement of microcirculation. Eur Heart J. 2010; 31:691–702. [PubMed: 20022872]
20. George RS, Sabharwal NK, Webb C, et al. Echocardiographic assessment of flow across continuous-flow ventricular assist devices at low speeds. J Heart Lung Transplant. 2010; 29:1245–52. [PubMed: 20688540]
21. Xydas S, Rosen RS, Ng C, et al. Mechanical unloading leads to echocardiographic, electrocardiographic, neurohormonal, and histologic recovery. J Heart Lung Transplant. 2006; 25:7–15. [PubMed: 16399524]
22. Ogletree ML, Sweet WE, Talerico C, et al. Duration of left ventricular assist device support: Effects on abnormal calcium cycling and functional recovery in the failing human heart. J Heart Lung Transplant. 2010; 29:554–61. [PubMed: 20044278]
23. Cowger J, Pagani FD, Haft JW, Romano MA, Aaronson KD, Kolias TJ. The development of aortic insufficiency in left ventricular assist device-supported patients. Circ Heart Fail. 2010; 3:668–74. [PubMed: 20739615]
24. Lang RM, Bierig M, Devereux RB, et al. Recommendations for chamber quantification: a report from the American Society of Echocardiography's Guidelines and Standards Committee and the Chamber Quantification Writing Group, developed in conjunction with the European Association of Echocardiography, a branch of the European Society of Cardiology. J Am Soc Echocardiogr. 2005; 18:1440–63. [PubMed: 16376782]
25. Nagueh SF, Appleton CP, Gillebert TC, et al. Recommendations for the evaluation of left ventricular diastolic function by echocardiography. J Am Soc Echocardiogr. 2009; 22:107–33. [PubMed: 19187853]
26. Lam KM, Ennis S, O'Driscoll G, Solis JM, Macgillivray T, Picard MH. Observations from noninvasive measures of right heart hemodynamics in left ventricular assist device patients. J Am Soc Echocardiogr. 2009; 22:1055–62. [PubMed: 19647406]
27. Serri K, Labrousse L, Reant P, Lafitte S, Roudaut R. Significant improvement of myocardial function following cardiac support device implantation: illustration by two-dimensional strain. Eur J Echocardiogr. 2006; 7:473–5. [PubMed: 16290131]
28. Cerqueira MD, Weissman NJ, Dilsizian V, et al. Standardized myocardial segmentation and nomenclature for tomographic imaging of the heart. A statement for healthcare professionals from the Cardiac Imaging Committee of the Council on Clinical Cardiology of the American Heart Association. Circulation. 2002; 105:539–42. [PubMed: 11815441]
29. Gibbons RJ, Christian TF, Hopfenspirger M, Hodge DO, Bailey KR. Myocardium at risk and infarct size after thrombolytic therapy for acute myocardial infarction: implications for the design of randomized trials of acute intervention. J Am Coll Cardiol. 1994; 24:616–23. [PubMed: 8077529]
30. Rocco TP, Dilsizian V, Strauss HW, Boucher CA. Technetium-99m isonitrile myocardial uptake at rest. II. Relation to clinical markers of potential viability. J Am Coll Cardiol. 1989; 14:1678–84. [PubMed: 2584556]
31. Altehoefer C, vom Dahl J, Messmer BJ, Hanrath P, Buell U. Fate of the resting perfusion defect as assessed with technetium-99m methoxy-isobutyl-isonitrile single-photon emission computed tomography after successful revascularization in patients with healed myocardial infarction. Am J Cardiol. 1996; 77:88–92. [PubMed: 8540466]
32. Udelson JE, Coleman PS, Metherall J, et al. Predicting recovery of severe regional ventricular dysfunction. Comparison of resting scintigraphy with 201Tl and 99mTc-sestamibi. Circulation. 1994; 89:2552–61. [PubMed: 8205664]
33. Dandel M, Weng Y, Siniawski H, et al. Heart failure reversal by ventricular unloading in patients with chronic cardiomyopathy: criteria for weaning from ventricular assist devices. Eur Heart J. 2011; 32:1148–60. [PubMed: 20929978]

34. Uriel N, Morrison KA, Garan AR, et al. Development of a novel echocardiography ramp test for speed optimization and diagnosis of device thrombosis in continuous-flow left ventricular assist devices: the Columbia ramp study. J Am Coll Cardiol. 2012; 60:1764–75. [PubMed: 23040584]
35. Myers TJ, Bolmers M, Gregoric ID, Kar B, Frazier OH. Assessment of arterial blood pressure during support with an axial flow left ventricular assist device. J Heart Lung Transplant. 2009; 28:423–7. [PubMed: 19416768]
36. Myers TJ, Frazier OH, Mesina HS, Radovancevic B, Gregoric ID. Hemodynamics and patient safety during pump-off studies of an axial-flow left ventricular assist device. J Heart Lung Transplant. 2006; 25:379–83. [PubMed: 16563964]
37. Ambardekar AV, Buttrick PM. Reverse remodeling with left ventricular assist devices: a review of clinical, cellular, and molecular effects. Circ Heart Fail. 2011; 4:224–33. [PubMed: 21406678]
38. Lamarche Y, Kearns M, Josan K, et al. Successful weaning and explantation of the Heartmate II left ventricular assist device. Can J Cardiol. 2011; 27:358–62. [PubMed: 21601774]
39. Akhter SA, D'Souza KM, Malhotra R, et al. Reversal of impaired myocardial beta-adrenergic receptor signaling by continuous-flow left ventricular assist device support. J Heart Lung Transplant. 2010; 29:603–9. [PubMed: 20202864]
40. Chokshi A, Drosatos K, Cheema FH, et al. Ventricular assist device implantation corrects myocardial lipotoxicity, reverses insulin resistance, and normalizes cardiac metabolism in patients with advanced heart failure. Circulation. 2012; 125:2844–53. [PubMed: 22586279]
41. Ogletree-Hughes ML, Stull LB, Sweet WE, Smedira NG, McCarthy PM, Moravec CS. Mechanical unloading restores beta-adrenergic responsiveness and reverses receptor downregulation in the failing human heart. Circulation. 2001; 104:881–6. [PubMed: 11514373]
42. Wohlschlaeger J, Levkau B, Brockhoff G, et al. Hemodynamic support by left ventricular assist devices reduces cardiomyocyte DNA content in the failing human heart. Circulation. 2010; 121:989–96. [PubMed: 20159834]
43. Manginas A, Tsiavou A, Sfyrakis P, et al. Increased number of circulating progenitor cells after implantation of ventricular assist devices. J Heart Lung Transplant. 2009; 28:710–7. [PubMed: 19560700]
44. Segura AM, Frazier OH, Demirozu Z, Buja LM. Histopathologic correlates of myocardial improvement in patients supported by a left ventricular assist device. Cardiovasc Pathol. 2011; 20:139–45. [PubMed: 20185339]
45. Saito S, Matsumiya G, Sakaguchi T, et al. Cardiac fibrosis and cellular hypertrophy decrease the degree of reverse remodeling and improvement in cardiac function during left ventricular assist. J Heart Lung Transplant. 2010; 29:672–9. [PubMed: 20188595]
46. Felkin LE, Lara-Pezzi E, George R, Yacoub MH, Birks EJ, Barton PJ. Expression of extracellular matrix genes during myocardial recovery from heart failure after left ventricular assist device support. J Heart Lung Transplant. 2009; 28:117–22. [PubMed: 19201335]
47. Mano A, Nakatani T, Oda N, et al. Which factors predict the recovery of natural heart function after insertion of a left ventricular assist system? J Heart Lung Transplant. 2008; 27:869–74. [PubMed: 18656800]

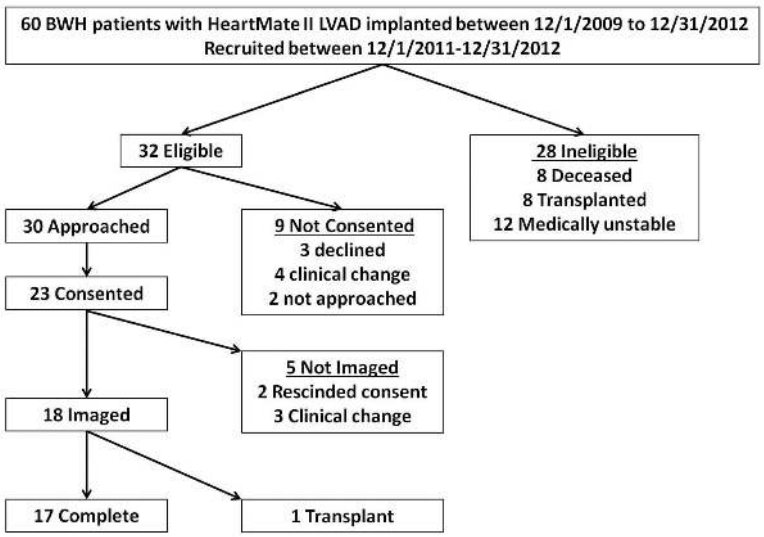

Figure 1.
Consort diagram of LVAD imaging study.

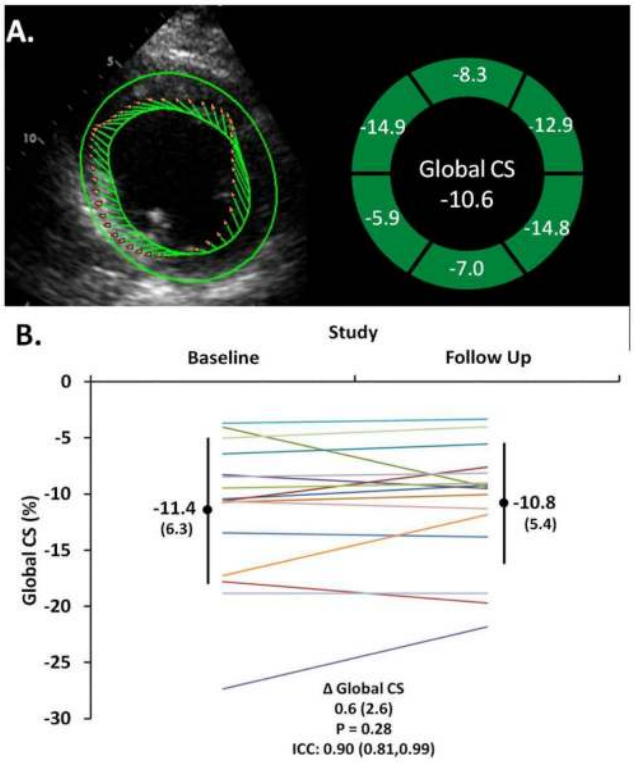

Figure 2.

A. Left ventricular systolic function was assessed with global circumferential strain (CS) from speckle tracking echocardiography at the mid ventricular level at the papillary muscles. B. At reduced LVAD support, LV systolic function (Global CS) is stable from baseline to follow up in chronically supported LVAD patients (each line represents a patient).

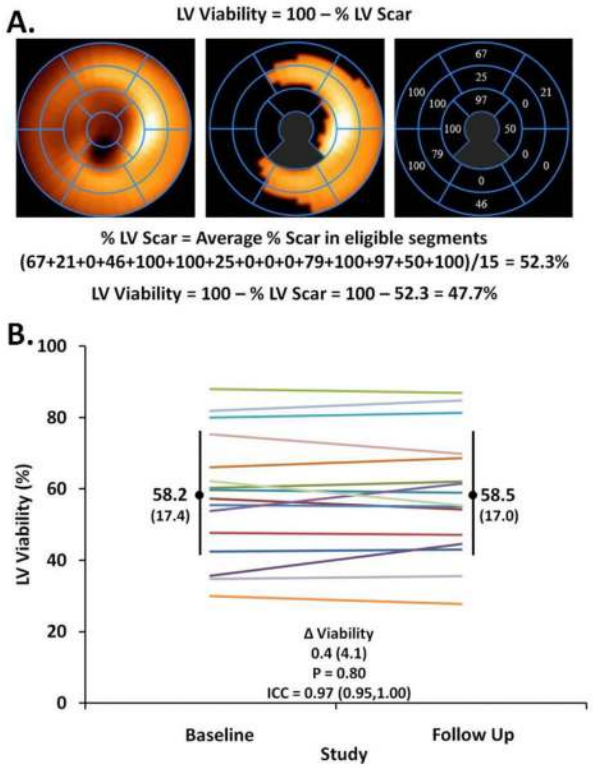

Figure 3.

A. At reduced LVAD support, global left ventricular viability was assessed by ^{99m}Tc Sestamibi SPECT imaging at a threshold of 55% of peak normalized counts, after exclusion of segments containing the LVAD cannula (gray zones). B. At reduced LVAD support, the extent of global LV viability was stable from baseline to follow up in chronically supported LVAD patients (each line represents a patient).

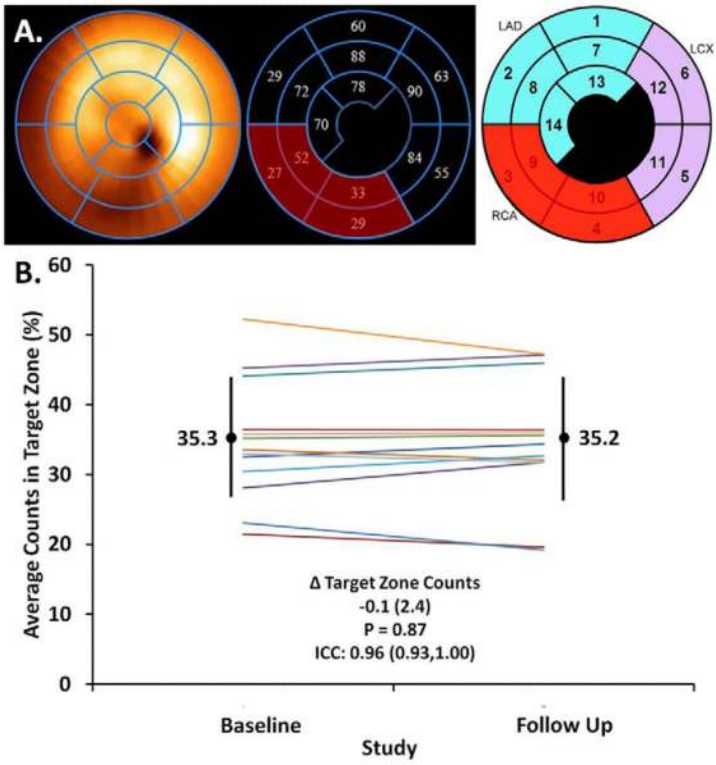

Figure 4.

A. At reduced LVAD support, the extent of regional LV viability was assessed by averaging peak normalized counts from ^{99m}Tc Sestamibi SPECT imaging in the target zone, defined as ≥2 contiguous segments with ≤55% of peak normalized counts within the same coronary distribution, after exclusion of segments containing the LVAD cannula. In this example of a patient with a history of a right coronary artery (RCA) STEMI, 4 segments (red) in the RCA territory comprised the target zone (average peak normalized counts = 35.3) B. At reduced LVAD support, the extent of regional LV viability in the target zones was stable from baseline to follow up in chronically supported LVAD patients (each line represents a patient).

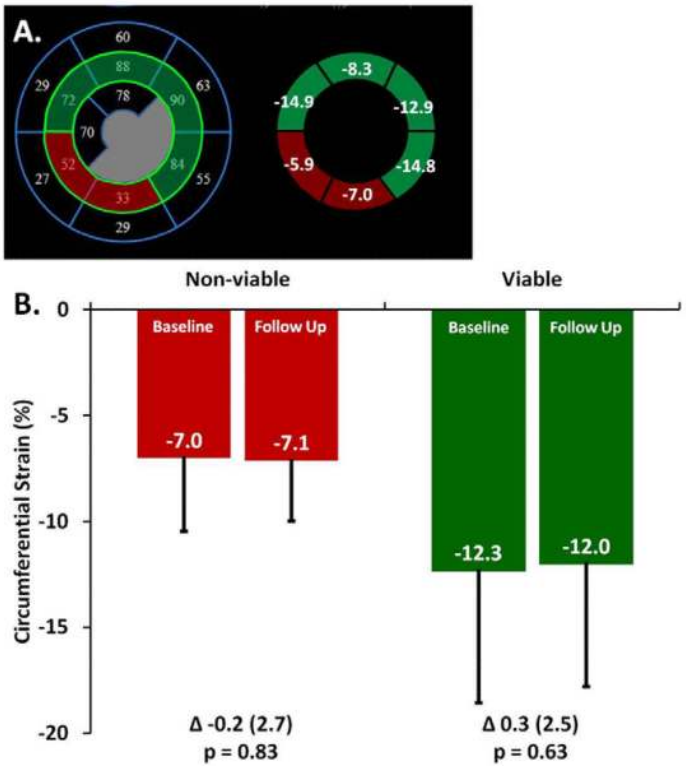

Figure 5.

The relationship between left ventricular viability and systolic function assessed by circumferential strain in chronically supported LVAD patients. A. The 6 mid LV segments were co-registered between SPECT (left) and echocardiographic (right) imaging in 15 patients. Each segment was categorized as viable (green) or non-viable (red) based upon >55% or ≤55% of peak normalized counts from ^{99m}Tc-Sestamibi SPECT imaging, respectively. Circumferential strain from speckle tracking echo was averaged in viable and non-viable segments. B. At reduced LVAD support, circumferential strain was compared between non-viable and viable segments over time and within studies (Baseline: Non viable vs viable p = 0.022; Follow Up: Non viable vs viable p = 0.017).

Table 1

Baseline characteristics of chronically supported clinically stable LVAD patients.

Characteristic	N=18
Age, years	61 (56,65)
Duration of HF, years	4.6 (2.4,8.5)
Duration of LVAD, months	6.9 (4.8,9.7)
Sex, male	15 (83)
Coronary Artery Disease	10 (56)
Prior Myocardial Infarction	9 (50)
Prior PCI	10 (56)
Prior CABG	4 (22)
Sarcoidosis	2 (11)
Hx/o Hypertension	7 (39)
Diabetes mellitus	7 (39)
Chronic kidney disease, eGFR < 60ml/min/ 1.73m^2	2 (11)
Body mass index, kg/m^2	27 (24,31)
Current smoker	2 (11)
ACEI or ARB	15 (83)
Beta blocker	18 (100)
Aldosterone antagonist	8 (44)
Hydralazine	1 (6)
Nitrates	1 (6)
Diuretics	11 (61)
Digoxin	1 (6)
Statin	13 (72)
Aspirin	18 (100)
Warfarin	18 (100)
Cardiac resynchronization therapy	8 (44)
Implantable cardioverter defibrillator	17 (94)

Data presented as median (IQR) or counts (%). HF = heart failure; LVAD = left ventricular assist device; PCI = percutaneous coronary intervention; CABG = coronary artery bypass grafting; eGFR = estimated glomerular filtration rate. ACEI = angiotensin converting enzyme inhibitor; ARB = angiotensin receptor blocker.

Table 2

Cardiac structure and function by echocardiographic imaging at ambulatory LVAD settings and reduced LVAD support.

Parameter	Ambulatory Settings	Reduced Support	Change	P
RPM	9200 (9200,9600)	6600 (6200,7400)	−2600 (−2200,−2800)	<0.001
Pulse Index	5.1 (4.2,5.9)	6.7 (6.3,6.9)	1.6 (0.8,2.5)	<0.001
Power, watts	6.2 (5.5,7.1)	2.9 (2.7,3.5)	−2.9 (−2.6,−4.2)	<0.001
Heart rate, bpm	78 (70,86)	73 (67,84)	0 (0,−5)	0.25
Doppler BP, mmHg	84 (78,88)	82 (80,90)	2 (−4,8)	0.44
Inflow Velocity, m/s	0.72 (0.62,0.89)	0.55 (0.46,0.64)	−0.18 (−0.06,−0.29)	<0.001
Outflow Velocity, m/s	0.81 (0.69,0.94)	0.80 (0.66,0.96)	−0.01 (0.05,−0.10)	0.62
LVEDD, cm	5.2 (4.3,5.7)	5.7 (4.6,6.5)	0.3 (0.2,0.9)	<0.001
LVESD, cm	4.7 (4.1,5.3)	5.3 (4.2,5.9)	0.5 (0.3,0.9)	<0.001
RVEDA, cm^2	25.0 (21.6,32.4)	20.2 (16.8,23.9)	−3.6 (−0.7,−7.6)	0.002
LV-GCS, %	−9.5 (−8.3 ,−13.9)	−10.5 (−8.3,−13.5)	−0.8 (1.6,−1.7)	0.76
LV-FAC, %	26 (20,29)	21 (17,31)	−1 (2,−3)	0.34
RV-FAC, %	40 (38,43)	37 (32,44)	−3 (1,−8)	0.33
E wave velocity, cm/s	71 (56,75)	75 (49,84)	5 (−6,14)	0.41
Average E' velocity, cm/s	9.0 (7.0,11.2)	8.3 (6.5,9.8)	−0.6 (0.2,−3.2)	0.07
LV filling pressures (E/e')	8.1 (6.1,8.6)	8.5 (6.4,9.7)	1.0 (0.0,2.5)	0.044
RV-RA gradient, mmHg	17 (16,23)	23 (17,29)	5 (−1,9)	0.018
RV Cardiac Output, L/min	5.2 (3.9,6.6)	4.3 (3.9,4.9)	−0.5 (0.1,−1.7)	0.15
PVR, Wood units	1.7 (1.4,2.1)	2.7 (2.3,3.2)	0.7 (0.4,1.4)	0.001

Data presented as median (IQR). P value from signrank test for paired data. RPM = rotations per minute; bpm = beats per minute, BP = blood pressure; LVEDD = left ventricular end diastolic diameter, LVESD = left ventricular end systolic diameter; RVEDA = right ventricular end diastolic area; LV-GCS = left ventricular global circumferential strain; LV-FAC = left ventricular fractional area change; RV-FAC = right ventricular fractional area change; RV-RA = right ventricular-right atrial; RV = right ventricular; PVR = pulmonary vascular resistance.

Table 3

The stability of cardiac structure and function by echocardiographic imaging at reduced LVAD support over time in chronically supported clinically stable LVAD patients.

Parameter	Baseline	Follow up	Δ	*P*	ICC
RPM	6600 (6200,7400)	6400 (6000,7000)	0 (−200,0)	0.10	0.85
Pulse Index	6.6 (6.3,6.8)	6.4 (5.7,6.8)	−0.3 (−0.7,0.4)	0.42	0.25
Power, watts	3.0 (2.7,3.6)	2.9 (2.7,3.7)	−0.1 (−0.4,0.4)	0.74	0.76
Heart rate, bpm	72 (66,84)	78 (69,83)	1 (−2,3)	0.43	0.38
Doppler BP, mmHg	82 (82,90)	88 (80,92)	0 (−4,10)	0.38	0.52
Inflow Velocity, m/s	0.55 (0.42,0.64)	0.49 (0.43,0.62)	−0.04 (−0.06,0.02)	0.21	0.99
Outflow Velocity m/s	0.76 (0.66,0.87)	0.82 (0.66,0.89)	0.06 (−0.04,0.10)	0.59	0.58
LVEDD, cm	5.6 (4.6,6.5)	5.6 (4.9,6.5)	−0.1 (−0.1,0.0)	0.22	0.98
LVESD, cm	5.2 (4.2,5.9)	5.2 (4.5,5.9)	0.0 (−0.1,0.1)	0.69	0.98
RVEDA, cm^2	20.2 (16.5,24.3)	22.1 (17.1,25.3)	1.4 (−1.0,3.5)	0.09	0.76
LV-GCS, %	−10.5 (−7.4,−15.4)	−9.5 (−7.9,−12.8)	0.4 (−0.5,1.1)	0.28	0.90
LV-FAC, %	21 (14,33)	21 (18,29)	−1 (−3,2)	0.64	0.89
RV-FAC, %	38 (33,44)	37 (32,44)	0.4 (−6,2)	0.64	0.59

Data presented as median (IQR). P value from signrank test for paired data. ICC = intraclass correlation coefficient; RPM = rotations per minute; bpm = beats per minute, BP = blood pressure; LVEDD = left ventricular end diastolic diameter, LVESD = left ventricular end systolic diameter; RVEDA = right ventricular end diastolic area; LV-GCS = left ventricular global circumferential strain; LV-FAC = left ventricular fractional area change; RV-FAC = right ventricular fractional area change.